Tidal current turbine evaluation using blade element momentum theory and computational fluid dynamics

Eng J. Yeo, David M. Kennedy and Fergal O'Rourke

Abstract— **Tidal current turbines are similar to wind turbines in terms of the principle of operation. However, due to higher fluid density, tidal current turbines need to withstand greater forces than wind turbines operating under similar conditions. Due to the similarity between the technologies, blade element momentum (BEM) theory, which was used largely for investigating and designing wind turbines, can also be used for tidal current turbines. Another method of performance evaluation of tidal current turbines is the use of computational fluid dynamics solvers such as Ansys CFX. This work investigated the use of BEM theory and Ansys CFX to evaluate the performance of a tidal current turbine. The use of BEM theory provided a computationally efficient and structured method to estimate the performance of a tidal current turbine compared to the computationally expensive CFD approach. However, the CFD approach offers a highly accurate modelling solution for evaluating the performance of a tidal current turbine. Importantly, further work in this domain will involve the integration of both modelling approaches which will offer high accuracy and increased computational efficiency.**

Keywords— **Blade Element Momentum Theory, Computational Fluid Dynamics, NACA 63(1)-8xx Series, NACA Airfoil Generator.**

I. Introduction

INTEREST in renewable energy has continued to grow steadily over the past years as various forms of energy conversion technologies are developed. Furthermore, this technological development has been initiated by the ever-growing demand for energy and the effects of climate change and carbon emissions. There are a large number of renewable energy technologies at an early stage of development, such as tidal energy. Regarding tidal current turbine technology, a number of projects have been developed with largely positive results. However, the technology is still some years behind established renewable energy technologies such as wind energy, solar energy, hydro energy, etc. but there are a number of recent studies in the literatures on the topic [1][2].

Open Hydro Ltd for example developed the open centre turbine and installed a 6m diameter prototype in May 2008 for testing. This turbine was connected to the UK grid. They have since developed turbines with higher power capacities such as the 1MW turbine installed in France and the 4MW turbine installed in Canada. The parent company of Open Hydro Ltd however has announced the cessation of its investment in 2018 causing the closure of Open Hydro Ltd [3].

Another recent tidal turbine technology developments have been made from the company called Sabella, this company has developed several prototypes such as the Sabella D10 and Sabella D03 with rotor diameter of 10m and 3m respectively. The Sabella company has scheduled a complete installation of a tidal current turbine farm in 2019 [2].

The potential of tidal energy however is enormous with numerous highly energetic sites worldwide. Additionally, tidal energy has the advantage over most other renewable energy types as it is predictable over large time-scales [4]. The density of water is much larger than air and thus the same power output from a wind turbine can be achieved with a smaller sized tidal current turbine (TCT) operating at lower freestream velocity.

There is a body of work in the literature showing that TCTs can potentially achieve higher power coefficients than wind turbines due to the blockage effects, i.e. confined tidal channels of the flow passage [5][6][7]. In addition to these studies, Belloni et al. have performed investigations of ducted and open-centre tidal turbines using blade element momentum (BEM) theory combined with computational fluid dynamics (CFD) [8]. Allsop et al. have similarly analysed ducted and open-centre tidal turbines using BEM theory validated with experimental data and compared to the coupled BEM-CFD method, which showed significant reduction in computational cost [9]. Heavey et al., Edmunds et al. and Batten et al. have carried out their studies based on the coupled BEM-CFD method [10][11][12].

ID: 1759; Track: Tidal Hydrodynamic Modelling

E. J. Yeo is with the Centre for Energy and Renewables at Dundalk Institute of Technology, Dundalk, County Louth, Ireland (e-mail: D00152871@student.dkit.ie)

D. M. Kennedy is with the Department of Mechanical Engineering, Dublin Institute of Technology, Bolton Street, Dublin 1, Ireland. (e-mail: david.kennedy@dit.ie)

F. O'Rourke is with the Centre for Energy and Renewables at Dundalk Institute of Technology, Dundalk, County Louth, Ireland (e-mail: fergal.orourke@dkit.ie)

TABLE I
ABBREVIATIONS AND NOMENCLATURE

Abbreviations		F	Tip loss factor
BEM	Blade element momentum	k	Turbulence kinetic energy per unit mass
CFD	Computational Fluid Dynamics	N	Number of blade elements
GGI	General Grid Interface	P	Power developed
MFR	Multiple Frames of Reference	p	Thermodynamic pressure
TCT	Tidal current turbine	p'	Modified pressure
TSR	Tip speed ratio	r_m	Element midpoint position
		S_M	Sum of body forces
Roman Notation		U	Free stream velocity
a	Axial induction factor	U_i, U_j, U_k	Vector of velocity
a'	Angular induction factor	V_{rel}	Relative velocity
B	Number of blades	x_i, x_j, x_k	Spatial distances
C_D	Drag coefficient		
C_L	Lift coefficient	*Greek Notation*	
C_T	Thrust coefficient	α	Angle of attack
C_{tan}	Tangential coefficient	γ	Twist angle
C_P	Power coefficient	μ	Laminar viscosity
dF_D	Local frag force	μ_{eff}	Effective viscosity
dF_L	Local lift force	μ_t	Turbulent viscosity
dF_N	Local normal force	λ	Tip speed ratio
dF_{tan}	Local tangential force	λ_r	Local tip speed ratio
dM	Local torque	Ω	Rotational speed
dP	Local Power	ϕ	Relative angle
dr	Blade element thickness	ρ	Fluid density

In this work, a BEM theory model and a CFD model have been developed to evaluate the performance of the tidal current turbine rotor, and the results are validated against experimental measurements found in the literature [13].

II. THEORY

A. The BEM algorithm

Blade element momentum (BEM) theory combines momentum theory and blade element theory and can be utilised to assess the performance of a tidal current turbine blade. Fundamental to the theory is dividing the blade into a number of elements each of which are analysed independently. Calculations of relative velocity, chord length, twist angle and angle of attack can then be performed on each element. Importantly, the lift and drag characteristics at each local element can then be determined. Thus, the forces and moments on each element can be obtained. By integrating the forces over the length of the blade, the torque and thrust can be determined. A detailed description of the BEM theory can be found in [14].

The hydrodynamic parameters on each blade element are illustrated in Fig. 1. The angles in the Fig. 1 consist of angle of attack, α, twist angle, γ, pitch angle, θ_p and relative angle of the tidal current flow, ϕ. Fig. 1. also includes the tangential force, dF_{tan}, lift force, dF_L, normal force, dF_N and drag force, dF_D. The horizontal dotted line in the figure represents the rotor plane. $r\Omega a' + r\Omega$ is the rotational speed parallel to the rotor plane and $(1\text{-}a)U$ is the freestream velocity at the rotor.

For the particular hydrofoil, the angle of attack, α can be used to determine the lift, C_L, and drag coefficients, C_D by interpolating experimental data or alternatively the lift and drag coefficients can be obtained through a software called XFoil. For this work, using the NACA 63(1)-8xx series hydrofoil, the lift and drag coefficients were obtained from Batten, W. M. J. et al. (2007) [12].

The tangential coefficient, C_{tan} of each element is calculated using (1).

$$C_{tan} = C_L \sin\phi - C_D \cos\phi \tag{1}$$

Using the calculated value of C_{tan} from (1), the local torque developed, dM is now calculated using (2) where ρ is the fluid density and dr is the thickness of the blade element.

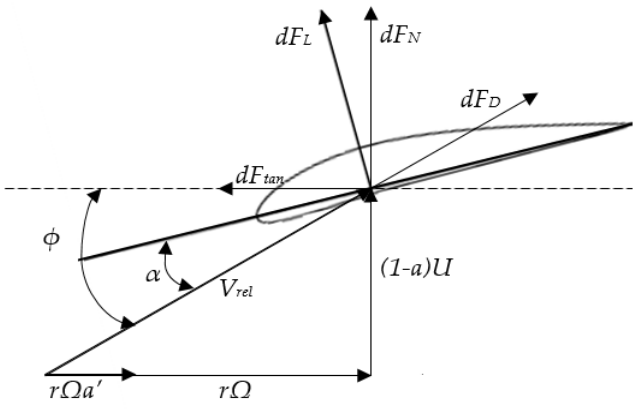

Fig. 1. Sectioned blade element diagram with angles, forces and velocities.

$$dM = \frac{1}{2} B\rho V_{rel}^2 C_{tan} c r_m dr \tag{2}$$

The overall power developed, P, by the blade for the specified tidal current speed is calculated by the sum of all elements for (3) where N is the number of blade elements.

$$dP = \Omega dM \tag{3}$$

$$P = \sum_{i=1}^{N} dP \tag{4}$$

The power coefficient, C_P of the TCT is calculated by using (4) divided by power available in the free stream as shown in (5).

$$C_P = \frac{P}{\frac{1}{2}\rho\pi R^2 U^3} \tag{5}$$

Blade tip loss effects occur as blade tip is approached. To quantify the blade tip losses, Prandtl's tip loss correction factor, F, can be used.

$$F = \left(\frac{2}{\pi}\right)\cos^{-1}\left[exp\left(-\left(\frac{\left(\frac{B}{2}\right)[1-(r_m/R)]}{(\frac{r_m}{R})\sin\phi}\right)\right)\right] \tag{6}$$

It is necessary to include the Glauert's correction model to account for the relationship between thrust coefficient and axial induction factor when the Prandtl's tip loss correction factor is included [15]. Equation (7) and (8) are Glauert's characteristic equation for thrust coefficient, C_T.

$$C_T = 4a\left(1 - \frac{1}{4}(5-3a)a\right) \quad a > 0.333 \tag{7}$$

Otherwise:

$$C_T = \frac{\sigma(1-a)^2(C_L\cos\phi + C_D\sin\phi)}{\sin^2\phi} \tag{8}$$

The axial induction factor, a and the angular induction factor, a' are determined using (9), (10) and (11).

$$a = \frac{1}{1 + \frac{4F\sin^2\phi}{\sigma C_L\cos\phi}} \quad C_T < 0.96 \tag{9}$$

Otherwise:

$$a = \left(\frac{1}{F}\right)\left[0.143 + \sqrt{0.0203 - 0.6427(0.889 - C_T)}\right] \tag{10}$$

$$a' = \frac{1}{\frac{4F\cos\phi}{\sigma C_L} - 1} \tag{11}$$

where solidity, σ, can be defined as the ratio of the area of the turbine rotor to the total swept area of the turbine. The local solidity at any specific radial position can be calculated using:

$$\sigma = \frac{cB}{2\pi r_m} \tag{12}$$

where c is the chord length and B is the number of blades.

B. Governing Equations – CFD Solver

The ANSYS CFX solver uses the Reynolds-averaged Navier-Stokes equations of momentum and mass conservation to approximate the flow field conditions around a tidal current turbine [12][16]. The continuity equation as shown in (13) and is solved together with the momentum conservation equation as shown in (14).

$$\frac{\partial\rho}{\partial t} + \frac{\partial}{\partial x_j}(\rho U_j) = 0 \tag{13}$$

$$\frac{\partial(\rho U_i)}{\partial t} + \frac{\partial(\rho U_i U_j)}{\partial x_j} = -\frac{\partial p'}{\partial x_i} + \frac{\partial}{\partial x_j}\left[\mu_{eff}\left(\frac{\partial U_i}{\partial x_j} + \frac{\partial U_j}{\partial x_i}\right)\right] + S_M \tag{14}$$

where U_i and U_j are the vectors of velocities of the fluid averaged over time, t, x_i and x_j are the spatial distance, S_M is the sum of body forces, μ_{eff} is the effective viscosity which is determined using (15) and p' is the modified pressure as defined in (16).

$$\mu_{eff} = \mu + \mu_t \tag{15}$$

$$p' = p + \frac{2}{3}\rho k + \frac{2}{3}\mu_{eff}\frac{\partial U_k}{\partial x_k} \tag{16}$$

where μ is the laminar viscosity, μ_t is the turbulence viscosity, p is the thermodynamic pressure, k is the turbulence kinetic energy per unit mass and U_k and x_k are the vector of velocity and spatial distance in their respective planar dimensions.

The k-ω shear stress transport (SST) model was chosen for its ability to model flow separation as well as its capability to account for the shear stress transport in adverse pressure gradient boundary layers [17].

ANSYS CFX uses the general grid interface (GGI) feature, a connection across a GGI attachment or periodic condition can be made using the control surface approach. The GGI algorithm is used to account for mismatched surfaces, for example when either side of an

interface do not match to form a well-defined physical connection. The solver also features Multiple Frames of Reference (MFR) based on the GGI technology which allows solving conditions where the domains are rotating relative to one another. These features, which reduce the complexity of the computational model, were utilised in this work [18].

III. METHODOLOGY

There are two main parts in the methodology for the current work, a steady BEM model and a CFD model. Fig. 2 details a simplified flow diagram of the model development for each numerical approach to evaluate the hydrodynamic performance of a TCT rotor.

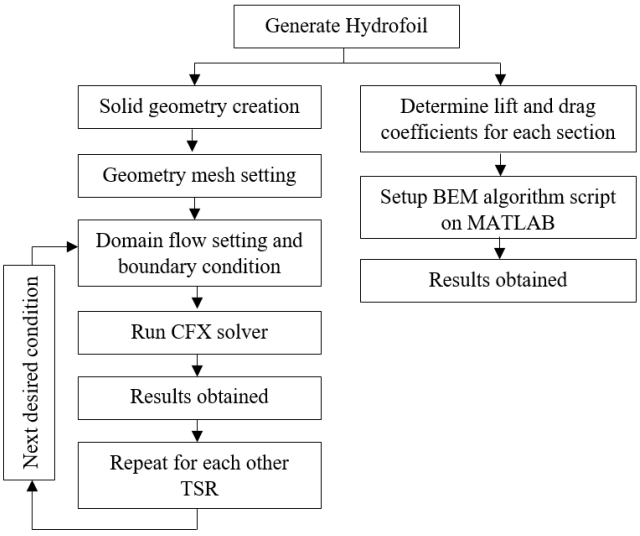

Fig. 2. Flow diagram of methodology for this work

The solution to the BEM model, based Equations (1) to (12), is solved for each blade element. The solution to the steady BEM theory model is obtained in seconds. The lift and drag coefficients were obtained from Batten et al. and are shown in Fig. 3 and 4 [19]. The CFD model, conversely, requires the development of a solid geometric representation of the turbine rotor, mesh development of the fluid domain and the application of the fluid flow setting.

C. Blade Geometry Creation

The hydrofoil sections were generated using the NACA Airfoil Generator that can be found in [20]. The blade was modelled using the NACA 63(1)-8xx series hydrofoil used in [19], the chord, thickness and pitch distribution are shown in Table II.

TABLE II
CHORD, TWIST ANGLE AND THICKNESS OF SPECIFIED TCT BLADE [19]

r/R	c/R	Twist (deg)	t/c (%)
0.20	0.1250	15.0	24.0
0.25	0.1203	12.1	22.5
0.30	0.1156	9.5	20.7
0.35	0.1109	7.6	19.5
0.40	0.1063	6.1	18.7
0.45	0.1016	4.9	18.1
0.50	0.0969	3.9	17.6
0.55	0.0922	3.1	17.1
0.60	0.0875	2.4	16.6
0.65	0.0828	1.9	16.1
0.70	0.0781	1.5	15.6
0.75	0.0734	1.2	15.1
0.80	0.0688	0.9	14.6
0.85	0.0641	0.6	14.1
0.90	0.0594	0.4	13.6
0.95	0.0547	0.2	13.1
1.00	0.0500	0.0	12.6

All 17 sections created using the NACA Airfoil Generator were exported in .txt file format so that they can be imported into the 3D solid geometry modeller (SolidWorks). Using the loft feature, the solid geometry of the TCT blade was generated and it was imported into ANSYS Workbench.

D. Mesh and flow setting

The following setup was prepared for the ANSYS CFX study. Due to the similarity in nature between wind turbines and TCTs, a full rotor CFD methodology for modelling the effects of wind turbine wake interactions on performance by Sturge et al., was utilised as a guideline [21]. The large domain extended 2, 3 and 2.5 diameters in the upstream, downstream and radial

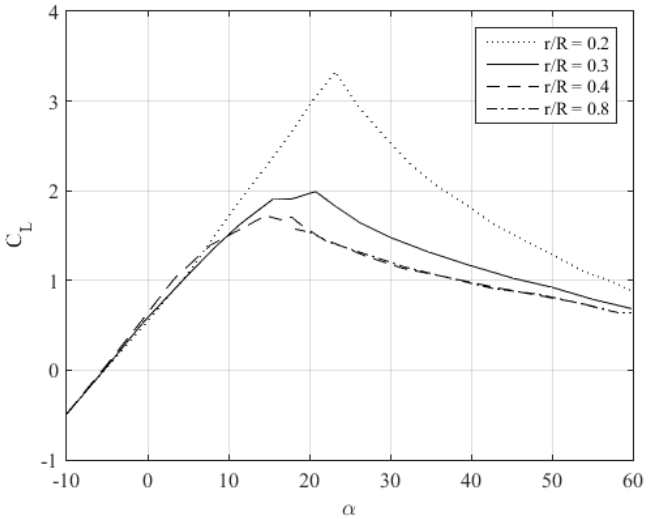

Fig. 3. Lift coefficients at four radial positions (Batten et al.) [19]

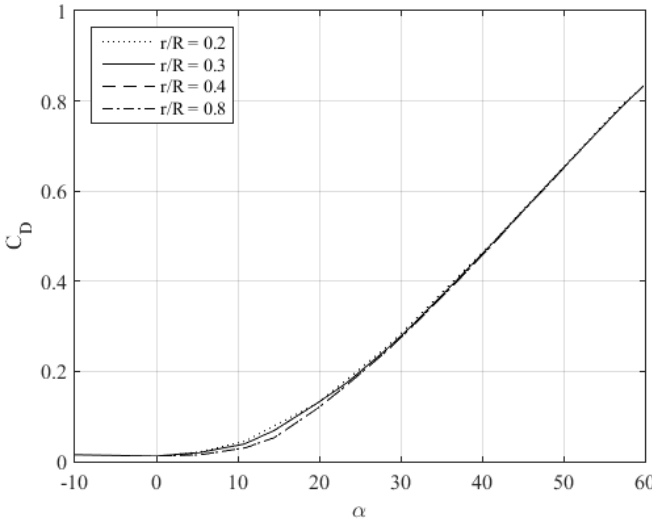

Fig. 4. Drag coefficients at four radial positions (Batten et al.) [19]

direction respectively. The rotating domain extended 0.6 diameters in the radial direction with a thickness of 0.1 diameters. As this was for a three-bladed TCT rotor, the domains were angled at 120°. The mesh was setup using fine relevance center and span angle center with a growth rate of 20%. Face meshing control was used on the wall of the blade in the rotating domain to generate a mapped mesh on the blade. Furthermore, this meshing technique enforces the number of specified divisions on the edge with a sizing control [22].

Rotational periodicity was specified on the flat areas on the sides. The k-ω shear stress transport (SST) turbulence model was used for the study. The angular velocity was set at 3.3 rad/s for the rotating domain. The wall of the blade was set to "no slip wall" and was assumed to have "smooth surface". As both the large and the rotating domains are fluid domains, they were setup using the "fluid-fluid" interface type. The large fluid domain is stationary while the smaller fluid domain has a rotating frame of reference, thus the "frozen rotor" option was chosen.

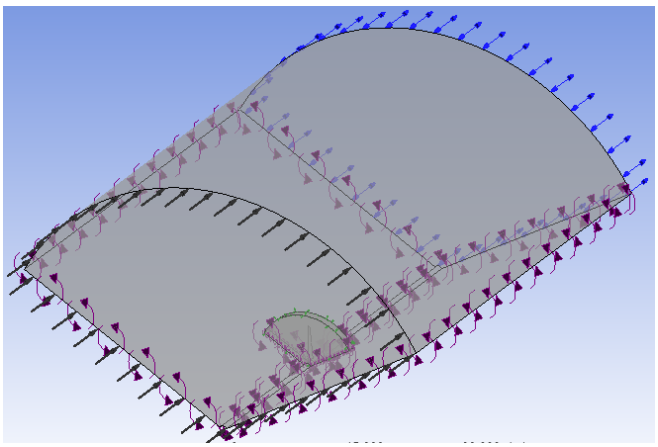

Fig. 5. Preview of CFX setup

The upstream inlet was set with a range of freestream velocities for tip speed ratios of 2 up to 10 on increments of 1 with turbulence option set at "Medium (Intensity = 5%)" for each study as that is the default intensity setting and it is the recommended option if there is no information about the inlet turbulence [23]. The downstream outlet was set as an entrainment opening with relative pressure of 0 Pa and turbulence option of "Zero Gradient".

IV. Results and Discussion

E. Mesh Comparison

Fig. 6 shows the mesh generated for the study with 3,000,000 elements and 500,000 nodes, the results are shown in Fig. 7 and 8. A mesh independence study was performed to compare the numerical accuracy of results. The study was performed using a Dell Inspiron 15R Laptop housing an Intel® Core™ i7-3612QM CPU @2.10GHz turbo boost up to 2.8 GHz with a 12.0 GB RAM setup. Table III was tabulated to show the significance of difference in the results for a TSR of 6 when different mesh settings were used as well as the time taken for each to converge for the same RMS residual target.

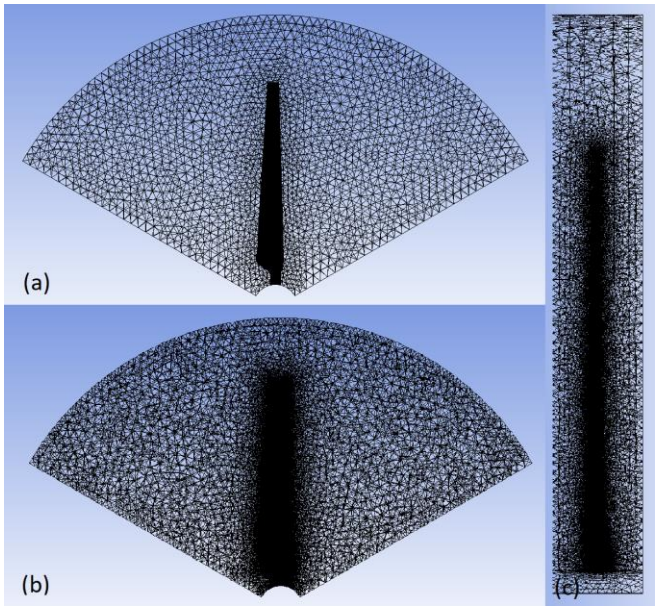

Fig. 6. Mesh generated at 3,000,000 elements and 500,000 nodes, (a) Front view of the mesh, (b) Cross-sectioned front view of the mesh, (c) Cross-sectioned side view of the mesh.

The experimental data obtained for a TSR of 6 in terms of power coefficient was approximately 0.45 and thrust coefficient was approximately 0.82. From the mesh independence study, 500,000 nodes in the mesh provided results with acceptable accuracy, 1,000,000 nodes took almost twice as long to run and provided a small difference of 3.38% in terms of C_P. Considering the mesh of only 580,000 elements and 100,000 nodes, the study did not produce reliable results. All four mesh settings however did not show any significant difference in terms of C_T.

F. Validation of Results

Fig. 8 and 9 show the results of the current study along with the experimental data of power and thrust coefficients obtained by Bahaj et al. [13] and the predicted data using the unsteady BEM model by O'Rourke et al. [24].

The steady BEM model, coded using MatLab, produced results instantly. ANSYS CFX however took

TABLE III
MESH STUDY ON TIP SPEED RATIO OF 6

Mesh	Number of Nodes	Number of Elements	C_P	C_T	ΔC_P (%)	ΔC_T (%)	Time Taken
1	100,000	580,000	0.3725	0.7134	0	0	1 hours 50 minutes
2	250,000	1,300,000	0.4129	0.7188	9.78	0.75	2 hours 42 minutes
3	500,000	3,000,000	0.4408	0.7243	6.76	0.76	5 hours 41 minutes
4	1,000,000	5,600,000	0.4562	0.7286	3.38	0.89	10 hours 4 minutes

approximately 2 hours for low TSRs and up to 14 hours for high TSRs in order to let the average root mean square (RMS) value to converge at a set residual target of 0.0001. In terms of power coefficient, the CFD model produced results that closely follow the curve of the experimental data at TSR of 6 and above. The steady BEM model closely predicted the performance of the turbine at low tip speed ratios, however, the accuracy could not be validated at low TSRs due to lack of experimental data. As the BEM model of Batten et al. included blockage correction factor, it accurately predicted the power coefficients between TSRs of 4 to 7.

In terms of thrust coefficient, all of the studies including the current work under-predicts the actual result.

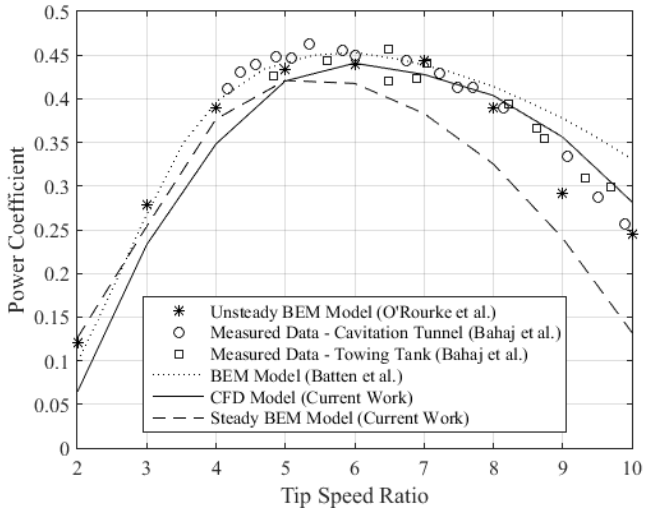

Fig. 7. Measured and estimated power coefficients versus tip speed ratio for NACA 63(1)-8xx series blade pitched at 5°.

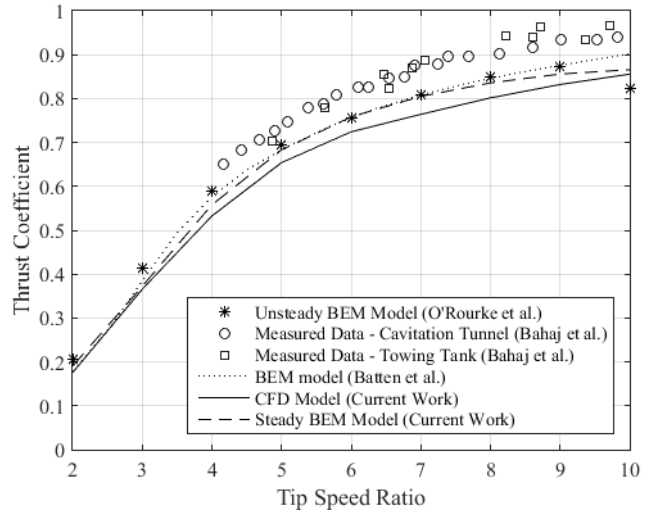

Fig. 8. Measured and estimated thrust coefficients versus tip speed ratio for NACA 63(1)-8xx series blade pitched at 5°.

V. CONCLUSION

The simple steady BEM model provides a quick solution to estimate the power and thrust coefficients, however it did not produce the result as accurate as the unsteady BEM model. As compared to the experimental data, the CFD model produced results with good accuracy at high TSRs, however it did not capture the thrust coefficients to the same degree of accuracy as the BEM model. Particular consideration was given to the number of elements in the region close to the wall of the turbine blade, i.e. concentrating a large amount of elements close to the blade to effectively capture the boundary layer. However, the most significant consideration of the modelling approach is the computational cost, whereas the BEM model has proved to be computationally efficient.

VI. FURTHER WORK

Due to the nature of this work, CFD required a significant computational time just to solve each condition. A more extensive mesh convergence study will be carried out to speed up the process of further works. Significant work will focus on achieving greater accuracy through meshing that includes y+ value studies as well as mesh quality.

A revised model based on the BEM-CFD method was presented by Edmunds et al. [25], which can produce more accurate results in predicting thrust and power as compared to other existing BEM-CFD models. Using experimental data where possible, an investigation can be undertaken by implementing this method to solve for complex flow conditions that includes the free surface, the sea floor and any other rigid boundaries.

In addition to these items, a combined study of the tidal energy resource and the blade performance will give greater insight into areas of improvement of turbine rotor design and array layout. Further work will be completed to compare the loading for different models, for example loading along the turbine blade span.

REFERENCES

[1] M. Z. Zainol, N. Ismail, I, Zainol, A. Abu, and W. Dahalan, "A review on the status of tidal energy technology worldwide," [Online] Available: https://www.researchgate.net/publication/317617074

[2] Z. Zhou, M. Benbouzid, J. Charpentier, F. Scuiller, and T. Tang, "Developments in large marine current turbine technologies – A review," *Renewable and Sustainable Energy Reviews*, vol. 71, pp. 852-858, May 2017. https://doi.org/10.1016/j.rser.2016.12.113, [Online]

[3] L. Siggins and A. O'Faolain, "Ocean Energy Europe 'disappointed' at OpenHydro liquidation" *The Irish Times*, Jul. 2018. [Online] Available: https://www.irishtimes.com/business/energy-and-resources/ocean-energy-europe-disappointed-at-openhydro-liquidation-1.3577586

[4] Green Match, "Enormous Potential of Tidal Energy and Wind Power in the UK", Jul. 2017. Available: https://www.greenmatch.co.uk/blog/2016/10/tidal-and-wind-energy-in-the-uk [Online]

[5] C. Garrett, and P. Cummins, "The efficiency of a turbine in a tidal channel" *Journal of Fluid Mechanics*, vol. 588, pp. 243-251, Oct. 2007. https://doi.org/10.1017/S0022112007007781, [Online]

[6] C. R. Vogel, R. H. J. Willden, and G. T. Houlsby, "Blade element momentum theory for a tidal turbine" *Ocean Engineering*, vol. 169, pp. 215-226, Dec. 2018. https://doi.org/10.1016/j.oceaneng.2018.09.018, [Online]

[7] S. Allsop, C. Peyrard, P. R. Thies, E. Boulougouris, and G. P., Harrison, "A validated BEM model to analyse hydrodynamic loading on tidal stream turbines blades" in *3rd AWTEC*, Singapore, 2016.

[8] C.S.K. Belloni, R.H.J. Willden, and G.T.Housby, "An investigation of ducted and open-centre tidal turbines employing CFD-embedded BEM" *Renew. Energy*, vol. 108, pp. 662-634, Aug. 2017. https://doi.org/10.1016/j.renene.2016.10.048 [Online]

[9] S. Allsop, C. Peyrard, P. R. Thies, E. Boulougouris, and G. P. Harrison, "Hydrodynamic analysis of a ducted, open centre tidal stream turbine using blade element momentum theory" *Ocean Engineering*, vol. 141 , pp. 531-542, Sep. 2017. https://doi.org/10.1016/j.oceaneng.2017.06.040, [Online]

[10] S. C. Heavey, S. B. Leen, and P. J. McGarry, "An efficient computational framework for hydrofoil characterisation and tidal turbine design" *Ocean Energy*, vol. 171, pp. 93-107. Jan. 2019. https://doi.org/10.1016/j.oceaneng.2018.10.032, [Online]

[11] M. Edmunds, R. Malki, A. J. Williams, I. Masters, T. N. Croft, "Aspects of tidal stream turbine modelling in the natural environment using a coupled BEM-CFD model" *International Journal of Marine Energy*, vol. 7, pp. 20-42, Sep. 2014. https://doi.org/10.1016/j.ijome.2014.07.001 [Online]

[12] W. M. J. Batten, M. E. Harrison, and A. S. Bahaj, "Accuracy of the actuator disc-RANS approach for predicting the performance and wake of tidal turbines" vol. 371, Feb. 2013. https://doi.org/10.1098/rsta.2012.0293, [Online]

[13] A. S. Bahaj, A. F. Molland, J. R. Chaplin, and W. M. J. Batten, "Power and thrust measurements of marine current turbines under various hydrodynamic flow conditions in a cavitation tunnel and a towing tank.", Mar. 2007. DOI:10.1016/j.renene.2006.01.012, [Online]

[14] M. O. L. Hansen, "Aerodynamics of Wind Turbines" London. 3rd Edition, 2015. [Online]. Available: https://doi.org/10.4324/9781315769981

[15] H. Glauert, "The analysis of experimental results in the windmill brake and vortex ring states of an airscrew" ARC-RM-1026, His Majesty's Stationery Office, London, 1926.

[16] CFX Documentation, "2.2.2.1. The k-epsilon Model in ANSYS CFX". Available: https://www.sharcnet.ca/Software/Ansys/17.0/en-us/help/cfx_thry/i1302321.html#i1302327, [Online]

[17] F. R. Menter, "Zonal two equation k-ω turbulence models for aerodynamic flows", AIAA-93-2906, 23rd Fluid Dynamics, Plasmadynamics, and Lasers Conference, Orlando, 1993. Available: https://doi.org/10.2514/6.1993-2906, [Online]

[18] CFX Document, "Chapter 3: GGI and MFR Theory". Available: https://www.sharcnet.ca/Software/Ansys/17.0/en-us/help/cfx_thry/i1304366.html, [Online]

[19] W. M. J. Batten, A. S. Bahaj, A. F. Molland, and J. R. Chaplin, "Experimentally validated numerical method for the hydrodynamic design of horizontal axis tidal turbines" *Ocean Engineering*, vol. 34, no. 7, pp. 1013-1020, May 2007. https://doi.org/10.1016/j.oceaneng.2006.04.008, [Online]

[20] NACA Airfoil Generator. Jan. 2019. [Online]. Available: https://github.com/adeharo9/NACA-airfoil-generator

[21] D. Sturge, D. Sobotta, and R.J. Howell, "A hybrid actuator disc – full rotor CFD methodology for modelling the effects of wind turbine wake interactions on performance" *Renew. Energy*, 80. pp. 525-537. https://doi.org/10.1016/j.renene.2015.02.053, [Online]

[22] CFX Document, "Face meshing control". Available: https://www.sharcnet.ca/Software/Ansys/16.2.3/en-us/help/wb_msh/ds_mapped_face_meshing.html, [Online]

[23] CFX Document, "2.4.2. Inlet (Subsonic)". Available: https://www.sharcnet.ca/Software/Ansys/16.2.3/en-us/help/cfx_mod/CHDIGAAJ.html, [Online]

[24] F. O'Rourke, F. Boyle, A. Reynolds, and D. M. Kennedy, "Hydrodynamic performance prediction of a tidal current turbine operating in non-uniform inflow conditions" http://dx.doi.org/10.1016/j.energy.2015.10.078, [Online]

[25] M. Edmunds, A. J. Williams, I. Masters, and T. N. Croft, "An enhanced disk averaged CFD model for the simulation of horizontal axis tidal turbines," *Renew. Energy*, vol. 101, pp. 67-81, Feb. 2017. https://doi.org/10.1016/j.renene.2016.08.007, [Online]